Laser and Particle Beams (2005), *23*, 143–147. Printed in the USA.

DOI: 10.1017/S0263034605050238

Generation of picosecond high-density ion fluxes by skin-layer laser-plasma interaction*

J. BADZIAK,[1] S. GŁOWACZ,[1] S. JABŁOŃSKI, P. PARYS,[1] J. WOŁOWSKI,[1] AND H. HORA[2]
[1]Institute of Plasma Physics and Laser Microfusion, Warsaw, Poland
[2]Department of Theoretical Physics, University of New South Wales, Sydney, Australia

(Received 30 November 2004; Accepted 9 December 2004)

Abstract

The possibilities of producing ultrahigh-current-density ps ion fluxes by the skin-layer interaction of a short ($\leq$ 1ps) laser pulse with plasma were studied using two-fluid hydrodynamic simulations, and the time-of-flight measurements. Backward-emitted ion fluxes from a massive (Au) target as well as forward-emitted fluxes from various thin foil targets irradiated by a 1-ps laser pulse of intensity up to 2×10^{17} W/cm^2 were recorded. Both the simulations and the measurements confirmed that using the short-pulse skin-layer interaction of a laser pulse with a thin pre-plasma layer in front of a solid target, a high-density collimated ion flux of extremely high ion current density ($\sim 10^{10}$ A/cm^2 close to the target), can be generated at laser intensity only $\sim 10^{17}$ W/cm^2. The ion current densities produced by this way were found to be comparable to (or even higher than) those estimated from recent short-pulse experiments using a target normal sheath acceleration mechanism at relativistic laser intensities. The effect of the target structure on the current densities and energies of forward-emitted ions is demonstrated.

Keywords: Ion fluxes; Laser; Picosecond pulses; Plasma

1. INTRODUCTION

High-peak-power laser generating short ($\leq$ 1ps) pulses enable the production of fast ion beams (Snavely *et al*., 2000; Clark *et al*., 2000; Badziak *et al*., 2001*a*; Borghesi *et al*., 2002; Hegelich *et al*., 2002; Zepf *et al*., 2003; Cowan *et al*., 2004; Pegoraro *et al*., 2004; Roth *et al*., 2005) with a potential to be applied in various fields of research including, in particular, high energy-density physics (Patel *et al*., 2003), and fast ignition of inertial fusion targets (Roth *et al*., 2001). However, these applications require high-density ion beams of extremely high current densities ($\sim 10^{10}$ A/cm^2 or higher), and of very short ion pulse duration (in the ps time scale). The above requirements are far beyond the present possibilities of conventional accelerators; they are attainable with the use of laser-driven ion sources. A possible way of producing ion beams with such extreme parameters is ballistic focusing (within a distance $\leq$ 1 mm) of energetic ions, driven by target normal sheath acceleration (TNSA) mechanism at relativistic laser intensities (Wilks *et al*., 2001; Patel *et al*., 2003).

In this paper, we consider another method, where the production of ps ion beams of ultrahigh current densities is possible in a planar geometry at subrelativistic laser intensities and at a low energy ($\leq$ 1 J) of the laser pulse. This method, hereinafter referred to as skin-layer ponderomotive acceleration (S-LPA), uses non-linear ponderomotive forces induced at the skin-layer interaction of a short laser pulse with a proper pre-plasma layer in front of a solid target (Badziak *et al*., 2004; Osman *et al*., 2004).

2. SKIN-LAYER PONDEROMOTIVE ACCELERATION OF IONS: A SIMPLIFIED PHYSICAL MODEL

A simplified model of production of high-density fast ion beams by the S-LPA mechanism was presented by Badziak *et al*. (2004). Very briefly, on the target surface the laser pre-pulse produces a pre-plasma layer of the thickness L_{pre}, at least several times smaller than the laser focal spot diameter d_f. The main short laser pulse interacts most intensely with the plasma in the skin layer near the surface of the critical electron density n_{ec} and the geometry of the inter-

Address correspondence and reprint requests to: Jan Badziak, Institute of Plasma Physics and Laser Microfusion, Henry Street 23, Warsaw 00-908, Poland. E-mail: badziak@ifpilm.waw.pl
*This paper was presented at the 28th ECLIM conference in Rome, Italy.

action is almost planar ($L_{pre} \ll d_f$). The high plasma density gradient in the interaction region induces two opposite non-linear forces which break the plasma and drive two thin ($\sim \lambda$) plasma blocks toward vacuum and toward the plasma interior, respectively (λ is the laser wavelength). As the density of the plasma blocks is high (the ion density $n_i \approx n_{ec}/z$, where z is the ion charge state) even at moderate ion velocities $v_i \sim 10^7$–10^8 cm/s, the ion current densities $j_s = zen_i v_i$ can be very high ($\sim 10^9$–10^{10} A/cm^2 or higher). The time duration of the ion current flowing out of the interaction region (being the ion source) is approximately equal to the laser pulse duration. Due to almost planar acceleration geometry, the angular divergence of the ion beam is small.

For subrelativistic laser intensities: $I \ll I_{rel} \approx 4.1 \times 10^{18}/\lambda^2$ (W/cm^2, μm), the ion energies, E_i, and the ion current densities, j_s, of the plasma blocks can be estimated from the equations (Badziak *et al.*, 2004):

$$E_i \approx 0.93 \times 10^{-16}\, sz\, I\, \lambda^2, \quad (\text{keV, W/cm}^2, \mu\text{m}) \tag{1}$$

$$j_s \approx 74\, (sz/\text{A})^{1/2} \lambda^{-1} I^{1/2,}\ (\text{A/cm}^2, \mu\text{m, W/cm}^2) \tag{2}$$

where $s = S$ for the forward-accelerated ions or $s = S$–1 for the backward-accelerated ions, S is the dielectric swelling factor and A is the atomic mass number. For instance, at $sz/\text{A} = 1$, a laser pulse of $\lambda = 1$ μm and of $I = 10^{17}$W/cm^2 produces the ion current density of $j_s \approx 2.3 \times 10^{10}$ A/cm^2.

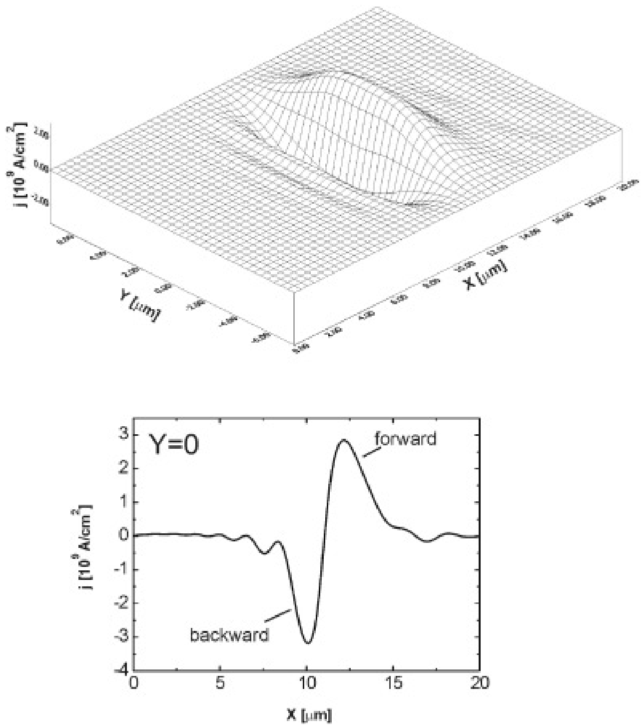

Fig. 1. Two-dimensional spatial distribution of the ion current density near the critical surface and its cross section at $Y = 0$ produced by a 200-fs laser pulse of intensity 10^{16} W/cm^2.

3. RESULTS OF NUMERICAL SIMULATIONS

The production of high-density ion fluxes by the S-LPA mechanism at subrelativistic laser intensities was investigated in detail using the advanced two-fluid plasma hydrodynamic model (Hora & Aydin, 1992; Boreham *et al.*, 1997). Both one- and two-dimensional codes were worked out for numerical calculations. An example of 2D calculations, performed for the case of 200-fs, 1.05-μm laser pulse of intensity 10^{16} W/cm^2 interacting with a hydrogen plasma ramp of linear initial profile, is shown in Figure 1. It illustrates the spatial distribution of the ion current density near the critical plasma surface and its cross section at $y = 0$ (along the laser beam axis). We can see the generation of the under dense plasma block moving against the laser (negative ion current densities) and the over dense plasma block behind the critical surface moving in the forward direction (positive ion current densities). The transverse distribution of ion current density (along the y-axis) follows the intensity distribution of the laser beam and the effective widths of the plasma blocks are close to the beam size.

The main conclusions from our numerical simulations are as follows: (a) the current densities and the velocities of backward-accelerated ions follow approximately a square-root dependence on the laser intensity as predicted by Eqs. (1) and (2); however, for the forward-accelerated ions, they increase faster with I and they attain higher values; (b) both for backward-accelerated and forward-accelerated ions there exist optimum values of the plasma density gradient scale length, L_n, and high plasma density gradients ($L_n < \lambda$) are preferable for the forward-accelerated ions; (c) the laser pulses of shorter wavelength produce ion fluxes of lower ion velocities but of higher current densities (Fig. 2, Eqs. (1) and (2)); (d) the current densities and the velocities of forward-accelerated ions continuously increase with an elongation of the laser pulse, but in the case of backward-accelerated ions, distinct maxima of the ion current densities and the ion velocities occur (Fig. 2); (e) at laser intensities $\sim 10^{16}$–10^{17} W/cm^2, the ion current densities attain values in the range of 10^9–10^{11} A/cm^2 in accordance with the simplified model of S-LPA.

4. RESULTS OF MEASUREMENTS

The experiment was performed with the use of Nd:glass CPA laser, generating a 1-ps, 1.05-μm pulse of a long-time scale (≥ 1 ns) intensity contrast ratio higher than 10^8 (Badziak *et al.*, 1997, 2001*b*). The intensity of the short lasting ($\sim 10^{-10}$ s) pre-pulse was $\sim 10^4$ times lower than the intensity of the main pulse (Badziak *et al.*, 2001*b*). For measurements of backward-accelerated ion fluxes, the linearly polarized laser beam was focused by an on-axis f/2.5 parabolic mirror, with a hole in the center, onto a massive Au target at an angle of 0° with respect to the target normal. The maximum intensity of the focused laser beam ($d_f \approx 20$ μm) was about 10^{17} W/cm^2. For the measurements of forward-

https://doi.org/10.1017/S0263034605050238 Published online by Cambridge University Press

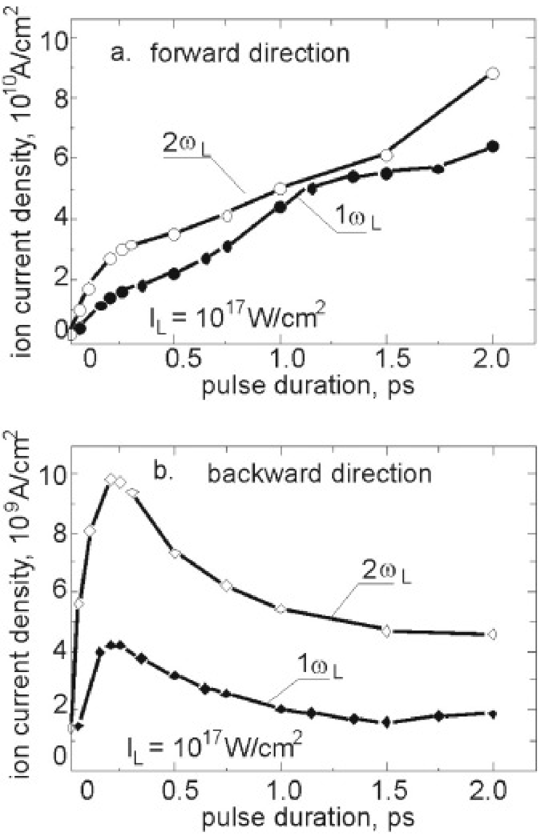

Fig. 2. The current densities of ions driven by a short laser pulse as a function of the laser pulse duration calculated for the first and the second harmonics of Nd:glass laser. $L_n/\lambda = 1$.

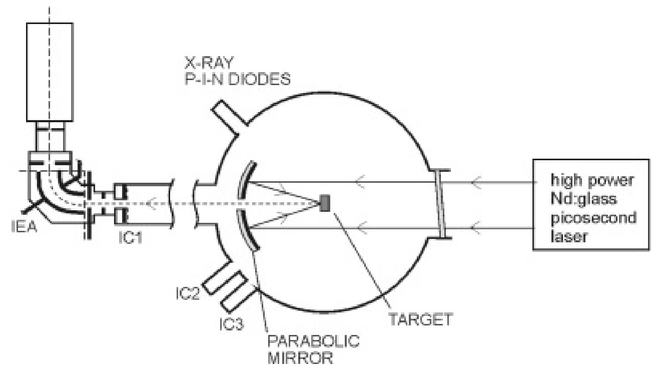

Fig. 3. Simplified scheme of the experimental arrangement. IEA–electrostatic ion-energy analyzer; IC1, IC2, IC3–ion collectors.

accelerated ion fluxes, the ps laser beam was focused by f/1 aspheric lens on a thin foil target normal to the target. The maximum laser intensity was 2×10^{17} W/cm^2. For both kinds of the targets used the short-lasting pre-pulse produced pre-plasma on the target surface of the thickness $L_{pre} \leq 5$ μm (Badziak *et al*., 2003, 2004).

The measurements of the ion flux parameters were performed with the use of ion collectors (ICs) and an electrostatic ion-energy analyzer (IEA) (Badziak *et al*., 2001*b*). The IEA and the ring ion collector (IC1) measured the backward-accelerated ions passing through the hole in the parabolic mirror along the target normal and the laser beam axis (Fig. 3). For a rough estimation of the angular distribution of ion emission, two additional collectors viewing the target at angles of 26° and 34° with respect to the target normal were applied. The forward-accelerated ions were recorded with the ICs and the IEA situated behind the thin foil target in the similar geometry.

For measurements of forward-accelerated ions, both single-layer and double-layer targets were used, and particularly: (1) polystyrene (PS) targets of the thickness, L_T, of 0.5 μm and 1 μm (marked as PS0.5 and PS1, respectively); (2) Al target of $L_T = 0.75$ μm (marked as Al0.75); (3) double-layer target with a 0.05-μm Au front layer and a 1-μm PS back layer (marked as Au0.05/PS1); (4) double-layer target with a 1-μm PS front layer and a 0.05-μm Au back layer (marked as PS1/Au0.05).

To estimate the fast ion current density at the source in the close vicinity of the target surface on the basis of our time-of-flight measurements we use the formula (Badziak *et al*., 2004):

$$j_s \approx Q_i/\tau_{is} S_s, \quad (3)$$

where: Q_i is the total charge of fast ions measured in the far expansion zone, τ_{is} is the duration of fast ion generation at the source, which is roughly equal to the laser pulse duration, $\tau_{is} \approx \tau_L$; S_s is the area of the fast ion source. We assume $\tau_{is} = \tau_L$, $S_s = S_f$ and $Q_i = Q_{IC1}$, where Q_{IC1} is the fast ion charge passing through the IC1 collector, seen within the angle of 3° from the source, and S_f is the focal spot area.

Our measurements of backward-accelerated ions, performed in the laser intensity range of 10^{16}–10^{17} W/cm^2, confirmed the linear dependence (Eq. (1)) of the mean ion energy on the intensity: $E_i \propto I^{1.02 \pm 0.18}$ as well as the square-root dependence (Eq. (2)) of the ion current density at the source on the intensity: $j_s \propto I^{0.57 \pm 0.08}$ with $j_s \approx 10^{10}$ A/cm^2 at $I = 10^{17}$ W/cm^2 (Badziak *et al*., 2004).

The measurements of forward-accelerated ions from thin foil targets revealed the fact that for all the targets used, only a single, highly collimated fast proton group, well separated from other, slower ion groups, is generated. The energy distributions of protons emitted from various thin foil targets as well as the proton current densities at the source, emitted within the 3° angle cone, are presented in Figure 4. The highest proton energies (both mean and maximum ones) were recorded for the Au0.05/PS1 target. In turn, the highest proton current densities ($> 2 \times 10^9$ A/cm^2) were achieved for the thinnest PS target and the lowest ones (for the Al target).

The ion current densities at the source achieved in our experiment ($j_s \sim 10^{10}$ A/cm^2) were found to be comparable to (or even higher than) those estimated from Eq. (3) for recent short-pulse experiments using the TNSA method at relativistic laser intensities. For instance, the data from the

https://doi.org/10.1017/S0263034605050238 Published online by Cambridge University Press

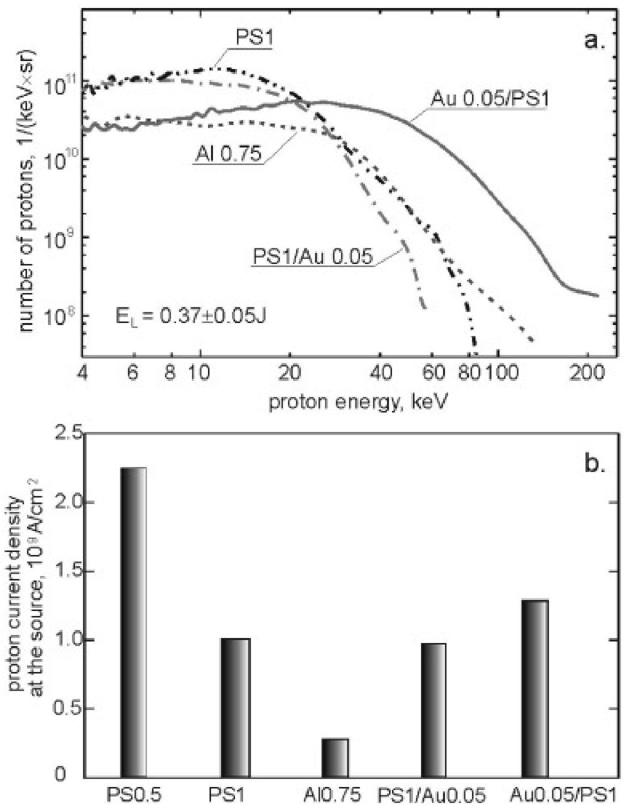

Fig. 4. The proton energy distributions (**a**) and the current densities at the source (**b**) of protons produced form various thin foil targets. $\tau_L = 1$ ps, $I_L = (1.2 \pm 0.2) \times 10^{17}$ W/cm^2.

petawatt experiment (Snavely *et al.*, 2000) result in a similar ($\sim 10^{10}$ A/cm^2) value of j_s, while j_s for the ballistic focused ion beam produced in the 100 TW/100 fs experiment (Patel *et al.*, 2003) was estimated to be at least a few times smaller.

5. CONCLUSIONS

It was shown that the S-LPA mechanism makes it possible to produce highly collimated high-density ion beams (plasma blocks) of extremely high ion current densities at the source, comparable to those produced by TNSA at significantly higher energy and power of a laser pulse. Apart from the simpler physics of the laser-plasma interaction, the advantage of S-LPA is the low energy of the driving laser pulses allowing the production of ultrahigh-current-density ion beams with a high repetition rate. It opens a prospect for unique tabletop experiments in high energy-density physics, ICF, or X-ray laser studies.

ACKNOWLEDGMENTS

This work was supported in part by the International Atomic Energy Agency in Vienna under Contract Number 11535/RO and by the State Committee for Scientific Research (KBN), Poland under Grant Number 1 PO3B 043 26.

REFERENCES

Badziak, J., Chizhov, S.A., Kozlov, A.A., Makowski, J., Paduch, M., Tomaszewski, K., Vankov, A.B. & Yashin, V.E. (1997). Picosecond, terawatt, all-Nd:glass CPA laser system. *Opt. Commun.* **134**, 495–502.

Badziak, J., Woryna, E., Parys, P., Platonov, K.Yu., Jabłoński, S., Ryć, L., Vankov, A.B. & Wołowski, J. (2001*a*). Fast proton generation from ultrashort laser pulse interaction with double-layer foil targets. *Phys. Rev. Lett.* **87**, 215001-1–215001-4.

Badziak, J., Makowski, J., Parys, P., Ryć, L., Wołowski, J., Woryna, E. & Vankov, A.B. (2001*b*). Intensity-dependent characteristics of a picosecond laser-produced Cu plasma. *J. Phys. D: Appl. Phys.* **34**, 1885–1891.

Badziak, J., Hora, H., Woryna, E., Jabłoński, S., Laśka, L., Parys, P., Rohlena, K. & Wołowski, J. (2003). Experimental evidence of differences in properties of fast ion fluxes from short-pulse and long-pulse laser-plasma interactions. *Phys. Lett. A* **315**, 452–457.

Badziak, J., Głowacz, S., Jabłoński, S., Parys, P., Wołowski, J. & Hora, H. (2004). Production of ultrahigh-current-density ion beams by short-pulses skin-layer laser-plasma interaction. *Appl. Phys. Lett.* **85**, 3041–3043.

Boreham, B.W., Hora, H., Aydin, M., Eliezer, S., Goldsworthy, M.P., Min, Gu., Gahatak, A.K., Lalousis, P., Stening, R.J., Szichman, H., Luther-Davies, B., Baldwin, K.G.H., Maddever, R.A.M. & Rode, A.V. (1997). Beam smoothing and temporal effects: Optimized preparation of laser beams for direct-drive inertial confinement fusion. *Laser Part. Beams* **15**, 277–295.

Borghesi, M., Campbell, D.H., Schiavi, A., Willi, O., Galimberti, M., Gizzi, L.A., Mackinnon, A.J., Snavely, R.D., Patel, P., Hatchett, S., Key, M. & Nazarov, W. (2002). Propagation issues and energetic particle production in laser-plasma interactions at intensities exceeding 10^{19}W/cm^2. *Laser Part. Beams* **20**, 31–38.

Clark, E.L. Krushelnick, K., Zepf, M., Beg, F.N., Tatarakis, M., Machacek, A., Santala, M.I.K., Watts, I., Norreys, P.A. & Dangor, A.E. (2000). Energetic heavy-ion and proton generation from ultraintense laser-plasma interactions with solids. *Phys. Rev. Lett.* **85**, 1654–1657.

Cowan, T.E., Fuchs, J., Ruhl, H., Kemp, A., Audebert, P., Roth, M., Stephens, R., Barton, I., Blazevic, A., Brambrink, E., Cobble, J., Fernández, J., Gauthier, J.-C., Geissel, M., Hegelich, M., Kaae, J., Karsch, S., Sage, G.P.Le., Letzring, S., Manclossi, M., Meyroneinc, S., Newkirk, A., Pépin, H. & Renard-LeGalloudec, N. (2004). Ultralow emittance, multi-MeV proton beams from a laser virtual-cathode plasma accelerator. *Phys. Rev. Lett.* **92** 204801-1–204801-4.

Hegelich, M., Karsch, S., Pretzler, G., Habs, D., Witte, K., Guenther, W., Allen, M., Blazevic, A., Fuchs, J., Gauthier, J.C., Geissel, M., Audebert, P., Cowan, T. & Roth, M. (2002). MeV ion jets from short-pulse laser interaction with thin foils. *Phys. Rev. Lett.* **89**, 085002-1–085002-4.

Hora, H. & Aydin, M. (1992). Suppression of stochastic pulsation in laser-plasma interaction by smoothing method. *Phys. Rev. A* **45**, 6123–6125.

Osman, F., Cang, Y., Hora, H., Cao, L.H., Liu, H., Badziak, J., Parys, P., Wolowski, J., Woryna, E., Jungwirth, K., Kralikova, B., Krasa, J., Laska, L., Pfeifer, M., Rohlena, K., Skala, J.& Ullschmied, J. (2004). Skin depth plasma front interaction mechanism with prepulse suppression to avoid relativistic self-focusing for high-gain laser fusion. *Laser Part. Beams* **22**, 83–87.

Patel, P.K., Mackinnon, A.J., Key, M.H., Cowan, T.E., Foord, M.E., Allen, M., Price, D.F., Ruhl, H., Springer, P.T. & Stephens, R. (2003). Isochoric heating of solid-density matter with and ultrafast proton beam. *Phys. Rev. Lett.* **91**, 125004-1–125004-4.

Pegoraro, F., Atzeni, S., Borghesi, M., Bulanov, S., Esirkepov, T., Honrubia, J., Kato, Y., Khoroshkov, V., Nishihara, K., Tajima, T., Temporal, M. & Willi, O. (2004). Production of ion beams in high-power laser-plasma interactions and their applications. *Laser Part. Beams* **22**, 19–24.

Roth, M., Cowan, T.E., Key, M.H., Hatchett, S.P., Brown, C., Fountain, W., Johnson, J., Pennington, D.M., Snavely, R.A., Wilks, S.C., Yasuike, K., Ruhl, H., Pegoraro, F., Bulanov, S.V., Campbell, E.M., Perry, M.D. & Powell, H. (2001). Fast ignition by intense laser-accelerated proton beams. *Phys. Rev. Lett.* **89**, 436–439.

Roth, M., Brambrink, E., Audebert, P., Blazevic, A., Clarke, R., Cobble, J., Cowan, T.E., Fernandez, J., Fuchs, J., Geissel, M., Habs, D., Hegelich, M., Karsch, S., Ledingham, K., Neely, D., Ruhl, H., Schlegel, T. & Schreiber, J. (2005). Laser accelerated ions and electron transport in ultra-intense laser matter interaction. *Laser Part. Beams* **23**, 95–100.

Snavely, R.A., Key, M.H., Hatchett, S.P., Cowan, T.E., Roth, M., Phillips, T.W., Stoyer, M.A., Henry, E.A., Sangster, T.C., Singh, M.S., Wilks, S.C., MacKinnon, A., Offenberger, A., Pennington, D.M., Yasuike, K., Langdon, A.B., Lasinski, B.F., Johnson, J., Perry, M.D. & Campbell, E.M. (2000). Intense high-energy proton beams from petawatt-laser irradiation of solids. *Phys. Rev. Lett.* **86**, 1769–1772.

Wilks, S.C., Langdon, A.B., Cowan, T.E., Roth, M., Singh, M., Hatchett, S., Key, M.H., Pennington, D., MacKinnon, A. & Snavely, R.A. (2001). Energetic proton generation in ultra-intense laser-solid interactions. *Phys. Plasmas* **8**, 542–549.

Zepf, M., Clark, E.L., Beg, F.N., Clarke, R.J., Dangor, A.E., Gopal, A., Krushelnick, K., Norreys, P.A., Tatarakis, M., Wagner, U. & Wei, M.S. (2003). Proton accelerations from high-intensity laser interactions with thin foil targets. *Phys. Rev. Lett.* **90**, 064801-1–064801-4.